Journal of Power Sources 196 (2011) 1909–1914

Contents lists available at ScienceDirect

Journal of Power Sources

journal homepage: www.elsevier.com/locate/jpowsour

Short communication

An analysis of the performance of an anaerobic dual anode-chambered microbial fuel cell

Min Hea Kim[a], Ifeyinwa J. Iwuchukwu[a,c], Ying Wang[b], Donglee Shin[a], John Sanseverino[b], Paul Frymier[a,b,c,*]

[a] Department of Chemical and Biomolecular Engineering, University of Tennessee, Knoxville, TN 37996, USA
[b] Center for Environmental Biotechnology (CEB), University of Tennessee, Knoxville, TN 37996, USA
[c] Sustainable Energy Education and Research Center, University of Tennessee, Knoxville, TN 37996, USA

ARTICLE INFO

Article history:
Received 1 August 2010
Received in revised form
17 September 2010
Accepted 20 September 2010
Available online 1 October 2010

Keywords:
Microbial fuel cell
Power generation
Dual anode chamber
Air cathode

ABSTRACT

The performance of a dual anode-chambered microbial fuel cell (MFC) inoculated with *Shewanella oneidesis* MR-1 was evaluated. This reactor was constructed by incorporating two anode chambers flanking a shared air cathode chamber in an electrically parallel, geometrically stacked arrangement. The device was shown to have the same maximum power density (approximately 24 W m^{-3}, normalized by the anode volume) as a single anode-, single cathode-chambered MFC. The dual anode-chambered unit generated a maximum current of 3.66 mA (at 50 Ω), twice the value of 1.69 mA (at 100 Ω) for the single anode-chambered device at approximately the same volumetric current density. Increasing the Pt-coated cathode surface area by 100% (12 to 24 cm^2) had no significant effect on the power generation of the dual anode-chambered MFC, indicating that the performance of the device was limited by the anode. The medium recirculation rate and substrate concentration in the anode were varied to determine their effect on the anode-limited power density. At the highest recirculation rate, 5 ml min^{-1}, the power density was about 25% higher than at the lowest recirculation rate, 1 ml min^{-1}. The dependence of the power density on the lactate concentration showed saturation kinetics with a half-saturation constant K_s on the order of 4.4 mM.

1. Introduction

Electricity generation using microbial fuel cells (MFC) has drawn significant attention recently as a new, potentially renewable source of energy [1]. MFCs are capable of generating electricity from waste and biomass, including sources of low or negative economic value such as wastewater [2–4]. The performance of MFCs depends on the system architecture, internal resistance, species and amount of bacteria on the anode, type of organic matter, chemical characteristics of the medium (pH, solution conductivity and chemical concentration) and the electrode surface characteristics [5–9]. Currently, single MFCs can produce a maximum working potential of only 0.3–0.8 V because of thermodynamic and practical constraints [10]. The connection of multiple MFCs in series or in parallel is therefore necessary to produce voltage or current high enough for practical application. Therefore, researchers have been developing and testing methods of scaling up single MFCs by stacking the individual MFC cells together in series or in parallel to achieve higher voltage or current [5,8]. Aelterman et al. [5] reported that the stack-in-series or stack-in-parallel circuit modes increased the system voltage or current (respectively), but that the stacked cells could not deliver power densities as high as a single cell, and that operation in series can lead to voltage reversal and energy loss. Oh et al. [8] investigated the causes of charge reversal and the impact of prolonged reversal on power generation using a two air-cathode MFC stack. They reported that voltage reversal was a result of fuel starvation leading to loss of bacterial activity, which could be restored by rapid feeding of the cell.

MFCs are being constructed using a variety of materials and an increasing diversity of configurations [11]. These different MFC configurations can be operated in varying conditions of temperature, electrode surface area, reactor size, electron acceptor and pH, all of which affect the MFC performance.

In this research study, replicates of a dual anode-chambered MFC reactor were constructed and operated to investigate the effect of the design on MFC performance when compared to a single anode-chambered system. For most MFCs, the cathode performance controls the power generation; however, the use of air

* Corresponding author at: Department of Chemical and Biomolecular Engineering, University of Tennessee, 419 Dougherty Engineering Building, Knoxville, TN 37996-2200, USA. Tel.: +1 865 974 4961; fax: +1 865 974 7076.
E-mail address: pdf@utk.edu (P. Frymier).

0378-7753/$ – see front matter © 2010 Elsevier B.V. All rights reserved.
doi:10.1016/j.jpowsour.2010.09.064

cathodes and platinum catalysts can reduce the ohmic, activation, and mass transport losses in the cathode [12]. This study considered air cathodes of two surface areas to determine if the system performance was limited by the cathode or the anode at the operating conditions of the study. The system was also studied to determine the effect of the medium recirculation rate and lactate concentration in the anode on the power density.

2. Materials and methods

2.1 MFC configuration

The dual anode-chambered MFC was constructed of three separate chambers: two anaerobic anode chambers and an air cathode chamber (Fig. 1). The design is a hybrid of the systems of Borole et al. [13], whose design uses small cylindrical anode chambers filled with carbon felt and air cathode chambers filled with carbon felt, and Wang and Han [10], who used MFC stacks with two anode chambers flanking a single air cathode chamber. The dual anodes were connected to the Pt-impregnated cathodes via a single graphite rod such that the dual anodes were electrically parallel (see Fig. 1). The anode (5 cm diameter and 2.5 cm long) and cathode (5 cm diameter and 1.25 cm long) chambers were fabricated from transparent polycarbonate material (a cylindrical Lexan tube). The anode and cathode chambers were separated by a PEM (proton exchange membrane, Nafion: 5 cm diameter, Alfa Aesar, Ward Hill, MA) fitted between two rubber gaskets. The anode chamber was completely filled with carbon felt, as in Borole et al. [13]. The liquid volume was 15 ml for one anodic compartment and the total anode reactor volume was 30 ml for the dual anode system. The single anode chambered MFC consisted of two chambers: an anaerobic anode chamber and an air cathode with the same dimensions as the dual anode-chambered MFC. In this configuration, the anode reactor volume was 15 ml. The PEM was pretreated by boiling it in a solution of deionized water and H_2O_2 (30%), followed by 0.5 M H_2SO_4 and deionized water, each for 1 h, and was then stored in deionized water prior to being used [14]. Solid graphite rods were inserted into the carbon felt of the anode and cathode chambers and the two anodes were connected in a parallel circuit using copper wire. The two anodes were separated from the cathode by a narrow gap of approximately 2 cm. Placing the anode and cathode close together has been shown to reduce MFC internal resistance [15–16]. The anodic compartments were filled with carbon felt to increase the surface area available for biofilm formation [17], thereby increasing the electron transfer rate and power density[18]. At the cathode, the graphite was used as the electron carrier for the final electron acceptor, oxygen; an air cathode was used for this design. Carbon cloth impregnated with platinum metal (Fuel Cell Store www.fuelcellstore.com, 2 cm × 3 cm) was used as the cathode material and was pressed directly against the PEM by the felt as in Borole et al. [13]. In one experiment, two different cathode surface areas (6 cm^2 and 12 cm^2) where used for each cathode electrode giving total cathode surface areas in the stacked dual anode systems of 12 cm^2 and 24 cm^2 respectively.

2.2 Inoculation and medium

A pure culture of *Shewanella oneidesis* MR-1 was used as the inoculum in the anode compartments of the MFCs. This organism is an exoelectrogenic bacterium because it transfers electrons outside the cell by producing nanowires [19] as well as soluble compounds such as flavins that can function as electron carriers [20]. The Defined Medium for *Shewanella* (DMS) from Galit Meshulam-Simon et al. [21] was used as the growth medium (pH = 6.8–7) and contained: 5.7 mM K_2HPO_4, 3.3 mM KH_2PO_4, 125 mM NaCl, 5.4 μM $FeCl_2 \times 4H_2O$, 5 μM $CoCl_2 \times 6H_2O$, 485 μM $CaCl_2 \times 2H_2O$, 5 μM $NiCl_2 \times 6H_2O$, 9 mM $(NH_4)2SO_4$, 0.2 μM $CuSO_4$, 1 mM $MgSO_4$, 1.3 μM $MnSO_4$, 1 μM $ZnSO_4$, 57 μM H_3BO_3, 67.2 μM Na_2EDTA, 3.9 μM Na_2MoO_4, 1.5 μM Na_2SeO_4, 2 mM $NaHCO_3$, and a vitamin mixture (1 l of medium contained 0.02 mg biotin, 0.02 mg folic acid, 0.1 mg pyridoxine HCl, 0.05 mg thiamine HCl, 0.05 mg riboflavin, 0.05 mg nicotinic acid, 0.05 mg DL-pantothenic acid, 0.05 mg p-aminobenzoic acid, 0.05 mg lipoic acid, 2 mg choline chloride, 0.01 mg vitamin B12). Filter-sterilized sodium DL-lactate at experiment-specific concentrations was used as the carbon source for cell growth and production of electricity. Cells were initially grown in LB medium with shaking at 33 °C overnight. Cells were then harvested by centrifugation (30,000 × *g* for 15 min) and washed three times in DMS solution with centrifugation after each wash. The washed cells were re-suspended in the DMS solution to the desired cell density (OD_{600} between 0.1 and 0.2).

2.3 MFC operation and measurement

A series of dual anode-chambered MFCs were operated at room temperature (approximately 22 °C) until stable power output was established. For these MFCs, the voltage across a load resistor was measured and recorded every minute by a data acquisition interface box (National Instruments, NI USD-6221) and a program written in Labview. Power output was determined to be stable when the voltage across the fixed resistance did not vary by more than 0.8% over a period of 5 h. Stable power output was typically achieved 5 days after inoculation. The voltage for three replicate reactors run simultaneously was measured and the average value was calculated. These averages were used to compare electricity production while varying experimental parameters.

The system's external resistance, substrate concentration, medium recirculation flow rate, and cathode surface area were varied in these experiments. Their effect on the operation of the dual anode-chambered MFCs was quantified by examining the cell potential, power, volumetric power density, internal resistance, and current. The system was operated with the medium continuously recirculated through a media bottle (Fig. 1a). The flow rate was controlled by a peristaltic pump. Fresh lactate was fed as a concentrated solution in the recirculating medium daily to bring the concentration in the system to the desired level for each experiment.

2.4 Analysis and calculations

The power P (W) was determined by measuring the voltage across an external resistor [11] using

$$P = \frac{E_{cell}^2}{R_{ext}} \quad (1)$$

where E_{cell} is the measured voltage (V) and R_{ext} the external resistance (Ω). In this study, the reactor liquid volume (specifically, the anode volume) was used as a normalizing factor for calculation of the power density (W m^{-3}).

The internal resistance is one of the critical system variables to consider in MFC construction; high reactor internal resistance limits the performance of the MFC by limiting current supply within the system [18]. In this study, both the polarization slope and power density peak methods were used to estimate the internal resistance. In the polarization slope method, the internal resistance of the cell, R_{int}, is calculated from the slope of plots of the cell voltage (E_{cell}) and current (I), as described by Logan et al. [11],

$$E_{cell} = OCV - IR_{int} \quad (2)$$

where OCV is the open circuit potential and the term IR_{int} represents the current-dependent overpotentials of the electrodes and ohmic losses of the system [11]. For the power density peak

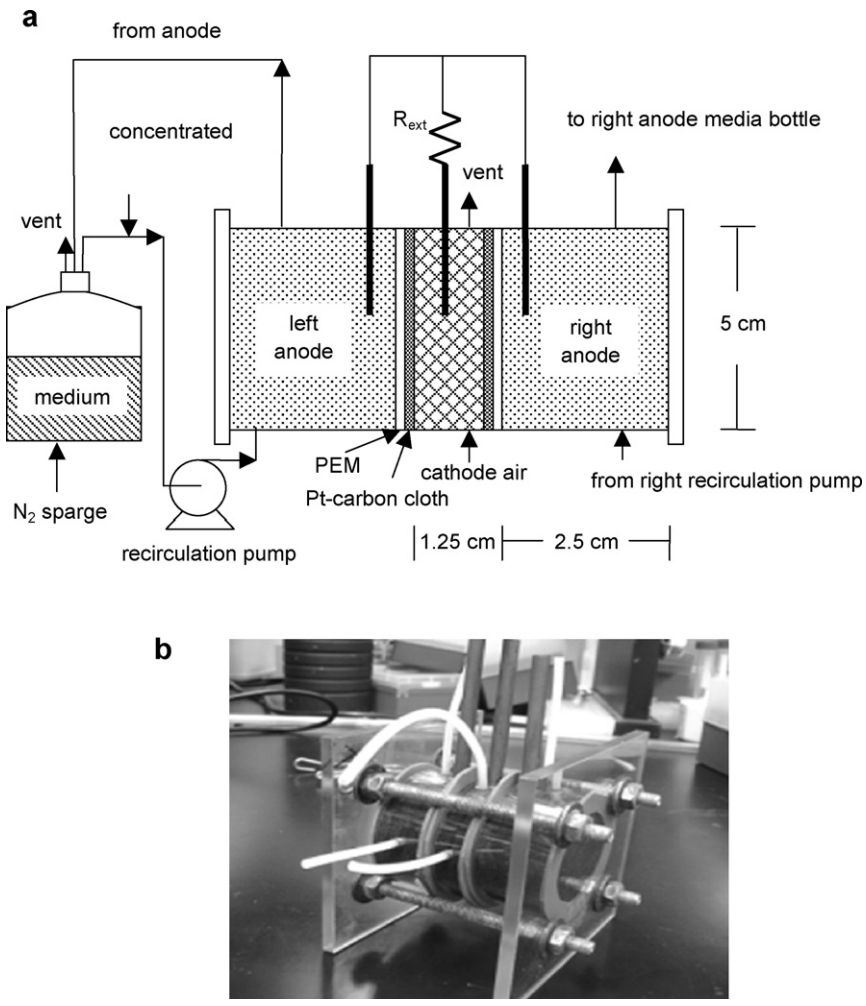

Fig. 1. Three dimensional view (a) and photograph (b) of a dual anode chambered MFC for electricity generation.

method, the maximum power for systems well described by Eq. (2) occurs at the point where the internal resistance is equal to the external resistance [18].

In this study, lactate was selected as the primary carbon source for *S. oneidensis* MR-1 to generate electric current in a minimal medium. Cell metabolism is a function of the substrate concentration on the biofilm covering the anode surfaces inside a stagnant fluid boundary layer so different lactate concentrations (5, 10, and 20 mM) in the medium and different medium recirculation rates (1, 3, and 5 ml min^{-1}) were tested and evaluated for their effect on the power output. The required substrate concentration in the system was maintained by continuously monitoring and analyzing the filter sterilized growth medium being re-circulated through the anodic chamber by high performance liquid chromatography (HPLC) (Waters, Alliance 2690 Analytical HPLC). The substrate consumption rate was determined daily from the changing lactate concentration. The reactor was operated as a fed-batch reactor, with the substrate added daily to bring the lactate concentration back to the desired level (5, 10, or 20 mM) and with the medium continuously recirculated by a small peristaltic pump to provide mixing in the anode. However, the substrate was added as a concentrated solution in a small volume (<5 ml) such that the system volume (approximately 200 ml) can be considered as in a pseudo-steady state. Therefore, the cell density increased slowly throughout the experiments. The cell growth rate was determined as a function of the substrate concentration by assuming that the growth rate is first order, which yields an exponential dependence of the cell density with time; this relationship can be described by the Monod equation:

$$\text{Specific growth rate, } \mu_g = \frac{\mu_m S}{K_s + S} \quad (3)$$

where S is the substrate concentration, K_s is the half-saturation constant, and μ_m is the maximum specific growth rate when $S \gg K_s$.

In most MFC systems, the power density is limited by the cathode, so the cathode area is frequently used to form a power density normalized by this area. Some studies also report the volumetric power density, normalized to the anode volume. To determine the most appropriate method of forming the power density, we investigated the effect of cathode surface area on power generation in our system; we used a rectangular shaped, platinized-carbon cloth as the cathode material and varied the surface areas of this cathode material. Two different cathode surface areas were used (Pt-impregnated carbon cloth rectangles of 4 cm × 3 cm and 2 cm × 3 cm, one for each cathode) and the power densities were compared to investigate cathode reactor performance.

3. Results and discussion

3.1 Power production using the dual anode-chambered MFC compared to a single anode-chambered MFC

The maximum power density (W m^{-3}) was obtained and used to compare the reactor performance of the dual anode-chambered

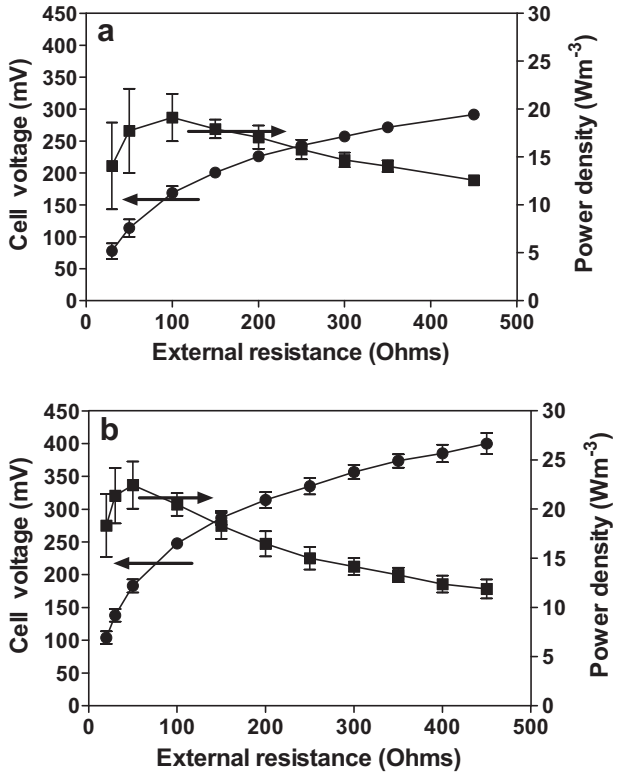

Fig. 2. Power density and cell voltage curves—by varying the external resistance we obtain the cell voltage and the volumetric power density as a function of resistance (a) single anode-chambered MFC and (b) dual anode-chambered MFC.

MFC with a single anode-chambered MFC. Both MFC systems produced stable and repeatable power generation within 120 h of inoculation with the reactor operated at an external resistance of 200 Ω at a lactate concentration of 10 mM and a recirculation rate of 5 mL/min. After voltage stabilization, both the open and closed circuit voltage were measured. The open circuit voltage (OCV) produced using the dual anode system was 0.65 ± 0.02 V, compared to 0.52 ± 0.01 V obtained by the single anode system. The average closed circuit voltage produced by the single anode system with a 200 Ω external resistor was 0.226 ± 0.01 V while 0.314 ± 0.02 V was obtained using the dual anode system (Fig. 2). The average voltage obtained using the single anode-chambered MFC was 39% lower than that produced by the dual anode-chambered MFCs at a fixed external resistance of 200 Ω. A polarization curve was generated using a variable resistor to vary the external resistance from 20 to 450 Ω. The power density from the single-anode MFC reached a maximum of 20.3 ± 4.43 W m^{-3}, producing a current of 1.69 mA (at 100 Ω) (Figs. 2 and 3). The MFC with dual anode-chambers generated 23.6 ± 2.25 W m^{-3} with a current of 3.66 mA (at 50 Ω). The power density was normalized to the anode liquid volume.

These volumetric power densities are comparable to reported values of 23 W m^{-3} using a two-cell MFC stack [1], 22.8 W m^{-3} using a single chamber stackable MFC reactor when four units connected in parallel and 14.7 W m^{-3} when connected in series [10], although considerably lower than the 56 W m^{-3} obtained by Borole et al. [13], on whose single anode-chambered design this reactor was based.

The current produced by the dual anode-chambered MFC was twice that produced by the single anode MFC, which was expected; the dual anode-chambered MFC is effectively two stacked single anode MFCs in parallel, but sharing a common external connection to the Pt-impregnated carbon felt cathodes of each cell.

In Fig. 3, the internal resistance is determined using the polarization slope method. The slopes of the polarization curve for single and dual anode MFC systems were linear over the ranges of 0.65–2.6 mA, Fig. 3(b_1) and 1.3–5.2 mA, Fig. 3(b_2), respectively. The internal resistance (slope) was determined to be 106 Ω for the single-anode MFC and 58.3 Ω for the dual anode-chambered MFC system, which is a reduction of 45% for the dual-anode system. For the power density peak method, the internal resistances was calculated to be 100 Ω for the single and 50 Ω for the dual anode-chambered system (Fig. 2), which is similar to that obtained using the polarization slope method. This result is consistent with the parallel connection of the two MFCs in this stacked geometry; the power (and current) density and cell voltage do not change when the stacked MFCs are connected in parallel through a common cathode chamber but with twice the anode volume of the single anode MFC. Therefore, the current and power are doubled for a fixed external resistance. The significance of this result is that this connection scheme does not appear to affect the microbial activity in the individual chambers. This result confirms those of others for different stacked systems although this is not true for series connection of stacked MFCs, where cells can undergo voltage reversal when connected in series [5,10].

3.2 Effect of cathode electrode surface area on MFC performance

The voltages produced using the same air-cathode system in the dual anode-chambered MFCs with two different total cathode surface areas (12 cm^2 vs. 24 cm^2) were compared and examined to determine the effect of cathode surface area. Increasing the surface area of the Pt-impregnated cathodes by 100% to 24 cm^2 (212.3 mV) had a negligible effect on power generation. An average maximum power density of 10.3 W m^{-3} was obtained with a 12 cm^2 cathode surface area and 10 W m^{-3} with 24 cm^2 when the MFCs were operated with a recirculation rate of 3 ml min^{-1} and a substrate concentration of 5 mM lactate. This result demonstrates that cathode surface area in the range of 12–24 cm^2 does not affect power generation in our system and that normalizing the power density with the cathode area would not be appropriate since the system is anode-limited. This was not the case for studies using the designs on which the dual anode-chambered system was based [10,13]. The review of Pham et al. [22] enumerates the losses that could potentially be limiting anode performance: low microbial activity at the anode, poor electron transfer rates at the anode, limited substrate mass transfer, and ohmic resistance of the membrane. The results of this experiment indicating the system is controlled by the anode performance, along with the long linear region seen in the polarization curve also points to the possibility of large ohmic losses in the anode [11], although it is not obvious what would cause these losses.

In order to determine if substrate mass transfer possibly resulting in low microbial activity was at least partially the cause of the limitation, we studied the effects of medium recirculation and lactate concentration on the power density of the dual anode system.

3.3 Effect of substrate concentration on MFC performance

An experiment was conducted in which the concentration of lactate in the feed to the reactor anode chamber was varied from 5 mM to 20 mM at a recirculation rate of 3 ml min^{-1}, and the voltage was recorded for a fixed external resistance. After each increase in the concentration of lactate, the voltage would fluctuate transiently before stabilizing at a new equilibrium value or returning to the previous value. After each change in the concentration of lactate, the reactors were allowed to reach stable voltage values. A plot of the resulting volumetric power density at each feed substrate concentration demonstrates saturation kinetics (Fig. 4). A maximum power density of P_{max}, 11.6 W m^{-3} was obtained using 5 mM lactate, while those using 10 mM and 20 mM lactate concentra-

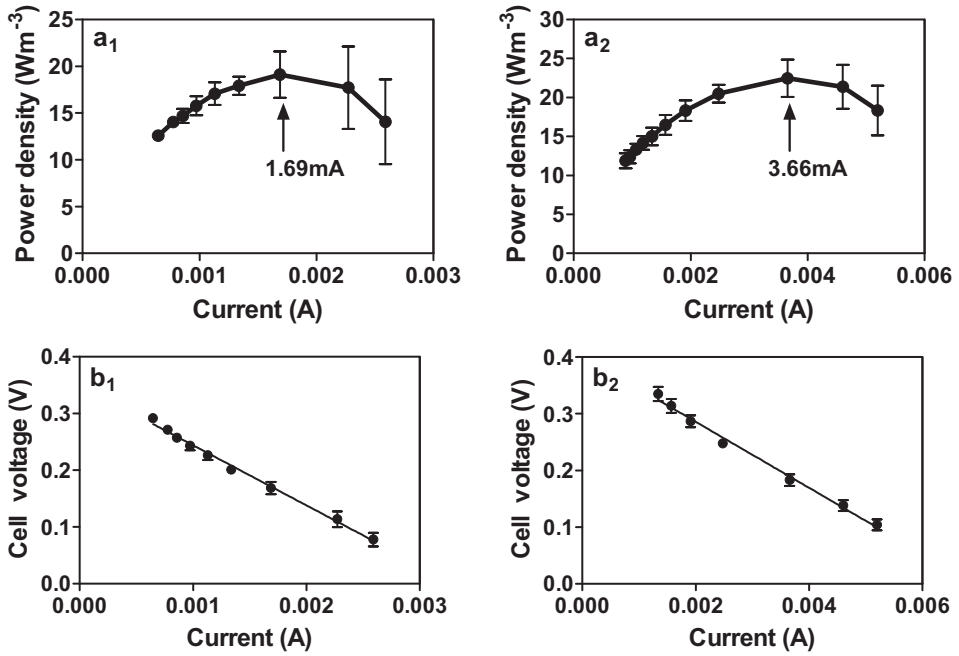

Fig. 3. Power density generated as a function of current (a_1) single anode-chambered MFC, (a_2) dual anode-chambered MFC, polarization curves—cell voltage versus current to obtain the polarization curve showing the regions of constant voltage drop (b_1) single anode-chambered MFC with best fit values; slope = −105.8 ± 4.196, *y* intercept = 0.3498 ± 0.006 and R^2 = 0.9622 and (b_2) dual anode-chambered MFC with best fit values; slope = −58.27 ± 2.142, *y* intercept = 0.4026 ± 0.007 and R^2 = 0.9933.

tions were P_{max} = 18.3 W m^{-3} and P_{max} = 18.5 W m^{-3}, respectively (Fig. 4). When fit to a model equation with Monod-like saturating behavior in which both the half-saturation and maximum power density values were selected based on a least-squares method (R^2 = 0.83), a half-saturation constant K_s of 4.42 mM was obtained for a maximum power density of 23.7 W m^{-3}. In Fig. 4, it appears that the measured power density may reach the maximum value before that predicted using the two-parameter model for saturating kinetics. Therefore, we explored the dependence of K_s on the value of the maximum power density in the kinetics model. The value of the maximum power density was fixed at values on either side of 23.7 W m^{-3}. Setting maximum power to 20 W m^{-3} and 30 W m^{-3} and then fitting the half-saturation constant results in a K_s value of 2.4 and 8.36 respectively. Based on Fig. 4, a K_s value on the order of 2.4–8.4 mM is appropriate. Therefore, a lactate concentration of 10 mM (significantly higher than K_s) was determined to be an appropriate concentration for efficient utilization of the substrate; at concentrations above this value, the increase in power generation is nominal.

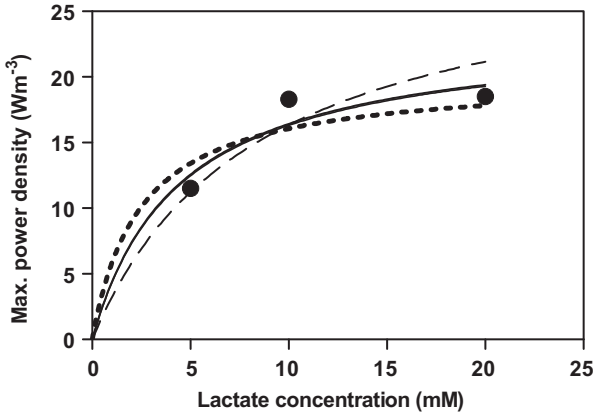

Fig. 4. Volumetric power density at each lactate concentration plot of saturation kinetics using a Monod-like kinetic model with K_s = 4.42 mM, R^2 = 0.83. Setting maximum power to 20 W m^{-3} (dotted line) and 30 W m^{-3} (dashed line) and then fitting the half-saturation constant results in a K_s value of 2.4 mM and 8.36 mM, respectively.

3.4 Effect of medium recirculation rate on power generation

Since nitrogen sparging and substrate addition occur outside the anode chamber, all mixing in the chamber is provided by recirculation through the anode to the medium bottle. Using continuous recirculating flow mode (Fig. 1a), the relationship between maximum power density and medium recirculation rate was investigated with lactate as the growth-rate limiting substrate of a culture of S. oneidensis MR-1. Here we considered the possibility that system hydrodynamics may affect power generation. We used a lactate feed concentration of 10 mM and medium recirculation rates of 1 ml min^{-1}, 3 ml min^{-1} and 5 ml min^{-1} and measured the maximum volumetric power density at each flow rate. The reactors used in this experiment employed 12 cm^2 of projected cathode surface area and 30 ml of total anode volume (15 ml in each anode chamber). Power densities of 17.7 ± 1.5 W m^{-3}, 18.3 ± 2.17 W m^{-3}, and 23.6 ± 2.25 W m^{-3} were achieved for recirculation rates of 1 ml min^{-1}, 3 ml min^{-1} and 5 ml min^{-1}, respectively. Higher recirculation rates could not be tested due to equipment limitations; the system could not withstand the higher system pressure. The medium recirculation rate of 5 ml min^{-1} produced approximately 22% higher power density than at a recirculation rate of 3 ml min^{-1} and 25% higher power density than at 1 ml min^{-1}. Other investigators have documented similar observations; Cheng et al. operated MFC reactors in batch and continuous flow modes and observed increased power density in the continuous flow mode [15]. They also observed that when their system was operated in continuous flow mode with flow through the anode, there was no detectable dissolved oxygen in the anode but observed 0.05–0.1 mg l^{-1} when the system was operated in batch mode. From these observations, they inferred that as the recirculation rate increases the amount of dissolved oxygen in the anode decreases. The presence of dissolved oxygen in the anode provides an alternate path for electrons, adversely affects the efficiency of the anode [15]. It is likely that higher recirculation rates in our reactors had a

similar effect since nitrogen sparging takes place outside the anode and oxygen that diffuses into the reactor through the gaskets that connect the sections of the MFC chambers lowers the power density.

Maximum growth rates of 0.03, 0.06, and 0.07 h^{-1} were calculated (assuming first order growth kinetics as discussed above) for medium recirculation rates of 1 ml min^{-1}, 3 ml min^{-1}, and 5 ml min^{-1}, respectively. These values are about the same at those in the literature for anaerobic growth of S. oneidensis MR-1 using either trimethylamine N-oxide (0.074 h^{-1}) or fumarate (0.87 h^{-1}) as the terminal electron acceptor [23]. The average substrate consumption rate for S. oneidensis MR-1 in the anaerobic dual anode system was approximately 5.5 mmoles lactate per liter of total liquid volume per day. We use total liquid volume to normalize the substrate degradation rate because cells were found in the recirculation sump bottle as well as attached to the felt in the anode. As noted earlier, it has been reported by Marsili et al. [20] that riboflavin secreted by MR-1 could function as an electron shuttle between the cells and the anode. In a different experiment an H-type and the single anode-chambered reactor where operated with the addition of 250 nM riboflavin to determine if reactor performance was enhanced. In MFC reactors operating at steady-state (i.e. constant voltage), supplementation of 250 nM riboflavin resulted in 20 mV and 30 mV improvement in maximum output voltage in the H-type system and the single anode-type reactor, respectively (data not shown). These results demonstrate that the supplementation of riboflavin at a very low concentration would increases MFC performance (by about 10% in this case). More importantly, this illustrates that plantonic cells are able to contribute to the power generation in our cells, either through transient contact or possibly through the use of nanowires or electron shuttle compounds, since they are known to produce both.

Note that the conditions above under which the system was found to be unaffected by halving the cathode area were for a recirculation flow rate of 3 ml min^{-1} and a lactate concentration of 5 mmol l^{-1}. Since both the lactate concentration and the recirculation flow rate affect the anode, we would expect to see some improvement of the anode if these values were closer to the higher values tested above. Assuming the improvements realized in increasing the flow rate and lactate concentration to their saturating values were additive, we would expect to see an improvement of around 90%, which is significant.

4. Conclusion

The dual anode-chambered MFC reactor configuration is electrically equivalent to two single anode-chambered systems in parallel (the volumetric power density is preserved). Since the volumetric power density is constant between single and dual anode-chambered MFCs, the internal resistance of a dual anode-chambered MFC is therefore about 45% lower than a single anode-chambered MFC with the same diameter but half the anode volume. In our system, the dual anode-chambered MFC displays a maximum volumetric power density of 23.6 W m^{-3} when operated in continuous recirculating flow mode under optimized values for the feed flow rate (5 ml min^{-1}) and substrate concentration (10 mmol l^{-1}).

The cathode area reduction experiment indicates that the dual anode-chambered MFC was anode limited; conditions of recirculation rate and lactate concentration for which the cathode reduction experiment was performed were found to be sub-saturating. The polarization curve data further indicates that the anode limitation was likely partially due to a high ohmic resistance in the anode. It is not clear what would cause this; the design of the reactor (close electrode spacing, high ionic strength buffer, high surface area-to-volume ratio) should minimize omhic resistance. Further electrochemical studies are recommended to elucidate the rate controlling processes in the cell.

Acknowledgements

The authors would like to acknowledge the support of the Joint Directed Research and Development Program at the University of Tennessee, Knoxville for this project, including support for Min Hea Kim and Dr. Ying Wang. Support for Ifeyinwa Iwuchukwu was provided by the Sustainable Energy Education and Research Center at the University of Tennessee, Knoxville.

References

[1] H. Liu, S.A. Cheng, B.E. Logan, Environmental Science & Technology 39 (2005) 5488–5493.
[2] Z. Du, Q. Li, M. Tong, S. Li, H. Li, Chinese Journal of Chemical Engineering 16 (2008) 772–777.
[3] Z. He, S.D. Minteer, L.T. Angenent, Environmental Science & Technology 39 (2005) 5262–5267.
[4] B. Min, J. Kim, S. Oh, J.M. Regan, B.E. Logan, Water Research 39 (2005) 4961–4968.
[5] P. Aelterman, K. Rabaey, H.T. Pham, N. Boon, W. Verstraete, Environmental Science & Technology 40 (2006) 3388–3394.
[6] J.R. Kim, S. Cheng, S.E. Oh, B.E. Logan, Environmental Science & Technology 41 (2007) 1004–1009.
[7] H. Liu, R. Ramnarayanan, B.E. Logan, Environmental Science & Technology 38 (2004) 2281–2285.
[8] S.E. Oh, B.E. Logan, Journal of Power Sources 167 (2007) 11–17.
[9] H. Liu, B. Logan, Abstracts of Papers of the American Chemical Society 228 (2004) U622–U1622.
[10] B. Wang, J.I. Han, Biotechnology Letters 31 (2009) 387–393.
[11] B.E. Logan, B. Hamelers, R.A. Rozendal, U. Schrorder, J. Keller, S. Freguia, P. Aelterman, W. Verstraete, K. Rabaey, Environmental Science & Technology 40 (2006) 5181–5192.
[12] H. Rismani-Yazdi, S.M. Carver, A.D. Christy, I.H. Tuovinen, Journal of Power Sources 180 (2008) 683–694.
[13] A.P. Borole, C.Y. Hamilton, D.S. Aaron, C. Tsouris, Biotechnology Progress 25 (2009) 1630–1636.
[14] S. Oh, B. Min, B.E. Logan, Environmental Science & Technology 38 (2004) 4900–4904.
[15] S. Cheng, H. Liu, B.E. Logan, Environmental Science & Technology 40 (2006) 2426–2432.
[16] M.M. Ghangrekar, V.B. Shinde, Bioresource Technology 98 (2007) 2879–2885.
[17] A.P. Borole, C.Y. Hamilton, T.A. Vishnivetskaya, D. Leak, C. Andras, J. Morrell-Falvey, M. Keller, B. Davison, Journal of Power Sources 191 (2009) 520–527.
[18] B.E. Logan, Microbial Fuel Cells Hoboken, N.J.: Wiley-Interscience, New Jersey, 2008.
[19] S.K. Lower, M.F. Hochella, T.J. Beveridge, Science 292 (2001) 1360–1363.
[20] E. Marsili, D.B. Baron, I.D. Shikhare, D. Coursolle, J.A. Gralnick, D.R. Bond, Proc. Natl. Acad. Sci. USA 105 (2008) 3968–3973.
[21] G. Meshulam-Simon, S. Behrens, A.D. Choo, A.M. Spormann, Applied and Environmental Microbiology 73 (2007) 1153–1165.
[22] T.H. Pham, P. Aelterman, W. Verstraete, Trends in Biotechnology 27 (2009) 168–178.
[23] Y.J. Tang, A.L. Meadows, J. Kirby, J.D. Keasling, Journal of Bacteriology 189 (2007) 894–901.